Environmental Science & Technology

Article

pubs.acs.org/est

Effects of Iron on Optical Properties of Dissolved Organic Matter

Brett A. Poulin,[†] Joseph N. Ryan,[†] and George R. Aiken*[,‡]

[†]Department of Civil, Environmental and Architectural Engineering, University of Colorado Boulder, Boulder, Colorado 80309, United States

[‡]United States Geological Survey, Boulder, Colorado 80303, United States

Supporting Information

ABSTRACT: Iron is a source of interference in the spectroscopic analysis of dissolved organic matter (DOM); however, its effects on commonly employed ultraviolet and visible (UV−vis) light adsorption and fluorescence measurements are poorly defined. Here, we describe the effects of iron(II) and iron(III) on the UV−vis absorption and fluorescence of solutions containing two DOM fractions and two surface water samples. In each case, regardless of DOM composition, UV−vis absorption increased linearly with increasing iron(III). Correction factors were derived using iron(III) absorption coefficients determined at wavelengths commonly used to characterize DOM. Iron(III) addition increased specific UV absorbances (SUVA) and decreased the absorption ratios (E_2:E_3) and spectral slope ratios (S_R) of DOM samples. Both iron(II) and iron(III) quenched DOM fluorescence at pH 6.7. The degree and region of fluorescence quenching varied with the iron:DOC concentration ratio, DOM composition, and pH. Regions of the fluorescence spectra associated with greater DOM conjugation were more susceptible to iron quenching, and DOM fluorescence indices were sensitive to the presence of both forms of iron. Analyses of the excitation−emission matrices using a 7- and 13-component parallel factor analysis (PARAFAC) model showed low PARAFAC sensitivity to iron addition.

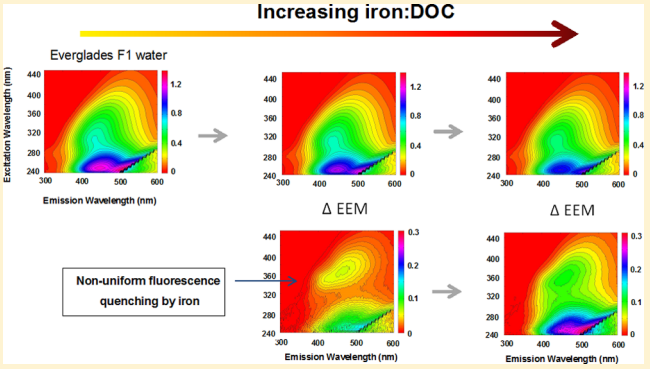

INTRODUCTION

The importance of dissolved organic matter (DOM) in biogeochemical, ecological, and engineering processes has been well-established over the past three decades. Optical measurements, namely, ultraviolet and visible (UV−vis) light absorption and fluorescence, have emerged as important analytical approaches to characterize DOM composition,[1−5] to infer DOM reactivity,[3] and as proxies for dissolved organic carbon (DOC) concentration.[6] Iron(III), which exhibits enhanced aqueous solubility in the presence of DOM,[7−9] is a recognized source of interference for both DOM UV−vis absorption[3,10−14] and fluorescence measurements.[2,15−18] However, the effects of iron on DOM optical properties are often ignored in studies reporting DOM optical data and warrant further investigation.

Aqueous iron(III) complexes[19] and iron(III) oxyhydroxide colloids[7] absorb light in UV regions utilized to characterize bulk DOM properties such as molecular weight[1] and aromatic carbon content.[3] For instance, iron(III) is known to interfere with the determination of specific UV absorbance at λ = 254 nm ($SUVA_{254}$), a proxy for DOM aromaticity.[3] Iron(III) interference can be eliminated by chemically reducing iron(III) to nonabsorbing iron(II).[13] However, the iron(III) reduction method may result in irreversible transformations of DOM upon reacting with the reductant[20] and does not provide a means to correct previously acquired data.

In contrast to UV−vis interferences, DOM fluorescence is known to be statically quenched by interactions with paramagnetic metal ions[21,22] including iron(III).[16−18,23] Ground-state metal−DOM complexes enhance intersystem crossing and other nonradiative processes that compete with DOM fluorescence.[16,24] Previous studies have shown that the degree of quenching by iron(III) varies by spectral region[17] based on differences in DOM composition.[18] These observations are of importance because qualitative fluorescence parameters relate the relative fluorescence of one peak or region to another.[2,4,25] Thus, elevated levels of iron(III) may represent a significant and unpredictable source of interference in determining fluorescence parameters, such as the fluorescence index (FI), commonly used to infer DOM source.[2] While sample acidification (pH 2) has been proposed to minimize metal quenching via metal complex dissociation,[2] the efficacy of this approach has not been demonstrated. Finally, earlier DOM fluorescence studies have not addressed potential interferences by iron(II), which is often present at elevated levels in anoxic porewaters and groundwater, and can be stabilized by DOM in well-oxygenated surface waters.[8]

Received: June 2, 2014
Revised: July 29, 2014
Accepted: August 1, 2014
Published: August 1, 2014

Table 1. Optical Properties of Dissolved Organic Matter (DOM), Hydrophobic Acid (HPoA) Fractions, and Surface Water Samples in the Absence of Iron

	Suwannee River HPoA (GA)	Everglades F1 HPoA (FL)	Everglades F1 water (FL)	Williams Lake water (MN)
[DOC][a] ($mg_C\ L^{-1}$)	2.5	2.3	5.0	4.5
$SUVA_{254}$[b] (L $mg_C^{-1}\ m^{-1}$)	4.49	4.40	3.45	1.17
FI[c]	1.17	1.26	1.35	1.49
S_R[d]	0.67	0.86	1.02	1.53

[a]Dissolved organic carbon concentration measured on DOM fractions and dilute surface water samples. [b]Specific ultraviolet absorbance at 254 nm.[3] [c]Fluorescence index (FI) defined as the emission ratio of 470 nm/520 nm at an excitation wavelength of 370 nm.[2] [d]The ratio of spectral slopes (S) between 275 and 295 nm and between 350 and 400 nm ($S_{275-295}$:$S_{350-400}$).[5]

In this study, iron(II) and iron(III) titration experiments were performed to assess the influence of iron on the absorbance and fluorescence of solutions containing two DOM fractions and two surface water samples with different optical properties. This work sought to establish an empirical iron(III) correction for UV−vis absorbance and characterize changes in parameters ($SUVA_{254}$, spectral slope ratio (S_R),[5] and absorption ratio at λ = 250 to 365 nm (E_2:E_3)[26]) commonly used to assess DOM composition and reactivity. Fluorescence efforts aimed to identify regions of excitation−emission matrix (EEM) fluorescence quenched by iron(II) and iron(III) across a range of DOM source materials, determine the sensitivity of parallel factor analysis (PARAFAC) models to iron interferences and quantify changes in prominent fluorescence indices. Finally, pH effects on DOM fluorescence in the presence and absence of iron were evaluated.

MATERIALS AND METHODS

Materials. DOM samples spanned a range of composition and optical properties associated with different source materials.[2,3,5] The hydrophobic organic acid (HPoA) isolates were obtained from the Suwannee River (GA) and the Everglades F1 site (FL) using XAD-8 resin.[27] Surface water samples from the Everglades F1 site (August 2010) and Williams Lake (MN; September 2010) were filtered (0.45 μm polysulfone filters) and refrigerated until use (≤16 days after collection). Everglades F1 and Williams Lake water had original DOC concentrations of 25.0 and 7.5 $mg_C\ L^{-1}$ and were diluted with high-purity water (≥18 MΩ cm) to final DOC concentrations of 5.0 and 4.5 $mg_C\ L^{-1}$, respectively, for iron titrations. Table 1 presents optical properties of DOM fractions and surface water samples. EEMs and background chemistry of DOM samples are presented in the Supporting Information (SI; Figure S1 and Table S1). The electron-donating capacities of Suwannee River HPoA and Williams Lake water were estimated using published values of International Humic Substances Society (IHSS) fractions[28] to evaluate changes in DOM redox state due to the reduction of added iron(III) (details in the SI). All acids were trace metal grade. All other reagents were ACS grade.

Iron stock solutions (0.56 g L^{-1}) were prepared with $Fe_2(SO_4)_3(H_2O)_5$ and $FeSO_4(H_2O)_7$ in 1 N HCl. The concentration and oxidation state of iron stock solutions were verified by inductively coupled plasma−optical emission spectrometry (ICP-OES; ARL model 3410+) and ferrozine analyses.[29] DOM stock solutions (50 $mg_C\ L^{-1}$) were prepared by dissolving DOM fractions in high-purity water and filtering through a 0.45 μm Supor membrane filter (Pall Corp.). Borosilicate glass jars (I-Chem 200 series) with Teflon-lined caps used in sample preparation were acid-cleaned (solution of 10% HCl and 10% HNO_3), rinsed with high-purity water, and baked at 450 °C for 4 h.

Iron Titrations. All solutions were prepared in a glovebox (5% H_2 and 95% N_2) with deaerated, high-purity water. Iron(III) reduction by H_2 was not observed in DOM-free solutions. Solution vessels were covered with aluminum foil. High-purity water and dilute surface water samples were deaerated by purging with ultrahigh-purity helium for 1 h. Experiments were designed to achieve an iron:DOC concentration ratio of 0−0.35 $mg_{Fe}\ mg_C^{-1}$ (0−1.5 mg L^{-1} iron) and have an absorbance at λ = 254 nm (A_{254}) < 0.2 cm^{-1} to minimize inner filter effects during fluorescence analysis.[2,30] Iron(III) concentrations exceeded the iron(III) binding capacity of the DOM.[31] Experimental solutions were prepared in duplicate at pH 6.7 (0.01 M $NaHCO_3$ buffer) and allowed to equilibrate for 24 ± 4 h at room temperature. The bicarbonate buffer minimized iron(II) oxidation by autocatalysis from iron(III) oxyhydroxide colloids.[7] Details on iron−DOM equilibration kinetics (SI Figure S2) and matrix effects are presented in the SI. In solutions containing DOM fractions, DOM was added from stock solutions to bring the DOC concentration to approximately 2.5 $mg_C\ L^{-1}$. For surface water samples, reagents were added to previously diluted waters. Iron was added to samples and the pH adjusted to 6.7 ± 0.2 with 0.1 M NaOH and 0.1 N HCl. Sample cuvettes were filled in the glovebox, capped, and transferred out for immediate spectrometric analysis. Additional iron(II) titrations were conducted with Suwannee River HPoA at seven pH values between 2 and 6.7 to assess UV interferences by iron(III) formed via iron(II) oxidation and pH dependence of fluorescence quenching. Experimental solutions, prepared in duplicate, contained 1 mM $NaClO_4$ and 2.5 $mg_C\ L^{-1}$ DOC. Solutions containing iron were spiked with 0.68 mg L^{-1} iron(II), and the pH was immediately adjusted to the target pH (±0.2). Solution pH was readjusted after 2 h equilibration time to adjust for changes resulting from iron(II) oxidation.

Sample Analysis. Sample pH (Beckman Coulter pHi410) and total iron and iron(II) concentrations were measured within 3 h of spectrometric analysis inside a glovebox. Total iron and iron(II) concentrations were measured using colorimetric methods (Hach Ferrover AccuVac ampules, Ferrous AccuVac ampules). Iron(III) concentrations were calculated as the difference between total iron and iron(II). Total iron and iron(II) concentrations were confirmed by a ferrozine assay[29] (difference between methods, ≤0.02 mg L^{-1}). DOC concentrations were determined by persulfate oxidation (OI Analytical, model 700).

A detailed account of all DOM optical measurements is provided in the SI. UV−vis absorption measurements were used to determine absorption coefficients (a_λ), $SUVA_{254}$,[3] E_2:E_3,[26] and S_R.[5] Iron(III) absorption coefficients (ε_λ; L mg^{-1}

cm^{-1}) were generated by a linear regression between decadic absorption coefficients corrected for DOM absorption (pH 6.7) and iron(III) concentration. Fluorescence EEMs are reported in Raman units (RU). Overall fluorescence intensity (OFI) was obtained by adding all fluorescence signals across the entire range of excitation wavelengths. Due to differences in fluorescence quantum yields between DOM samples, fluorescence data at pH 6.7 are presented as the relative fluorescence (OFI/OFI_0), with OFI and OFI_0 determined in the presence and absence of iron, respectively. Total iron concentrations were used to determine iron:DOC concentration ratios. Two fluorescence indices were determined: FI and the redox index (RI), the latter proposed to infer DOM redox state.[32] EEMs were analyzed using previously established 7-component[33] and 13-component PARAFAC models.[4] Rayleigh scatter was determined at excitation/emission wavelengths ($\lambda_{ex}/\lambda_{em}$) 350 nm/350 nm to assess the formation of iron(III) oxyhydroxide colloids in experimental solutions.[23,34] EEM subtractions were conducted to represent the fluorescence quenched (EEM_{FQ}) upon iron addition using the following:

$$EEM_{FQ} = EEM_0 - EEM \quad (1)$$

where EEM_0 and EEM were determined in the absence and presence of iron, respectively. EEMs of fluorescence reduction (EEM_{FR}) upon acidification in the absence of iron were determined using the following:

$$EEM_{FR} = EEM_{pH\,6.7} - EEM_{pH} \quad (2)$$

where $EEM_{pH\,6.7}$ was determined at pH 6.7 and EEM_{pH} was determined at the specified pH.

RESULTS

Iron Oxidation State in Experimental Solutions. Solutions with added iron(II) (pH 6.7; 0.01 M $NaHCO_3$) showed >90% preservation of the iron(II) oxidation state. These solutions showed little change in Rayleigh scattering (SI Figure S3a). Experiments conducted at different pH values in the absence of carbonate showed low levels of iron(II) oxidation at pH < 4 and considerable iron(II) oxidation at pH > 4 (SI Figure S4a). Rayleigh scattering of these solutions increased at pH > 4 due to iron(II) oxidation and iron(III) hydrolysis (SI Figure S3c). Samples prepared at pH 5 exhibited a pH increase to values of 6.0 and 6.3. Due to differences in iron oxidation state and pH between experimental replicates, single data points are presented for this experiment.

At pH 6.7, as much as 45% of added iron(III) was reduced to iron(II) at low iron(III) concentrations (0.11 mg L^{-1}). The extent of iron(III) reduction varied between DOM samples and with added iron(III) but did not exceed 0.07 mg L^{-1} in any sample. Dark reduction by DOM is likely responsible for this observation.[15,35] Because DOM fluorescence properties are redox-sensitive,[4,36] potential inadvertent oxidation of DOM due to iron(III) reduction was evaluated by comparing estimates of DOM electron-donating capacity to the electron equivalents of iron(III) reduction (details in the SI). DOM electron-donating capacities always exceeded the electron equivalence of reduced iron(III) (e.g., ≥6-fold). These analyses provide evidence that the oxidation of electron-donating moieties in DOM due to iron(III) reduction was likely insufficient to change DOM fluorescence properties. Aside from Williams Lake water, Rayleigh scattering of the iron(III) titrations did not exceed a 2-fold increase at high iron(III) (SI Figure S3b), indicating low levels of iron(III) oxyhydroxide colloids.[23,34] Williams Lake water solutions exhibited an 8-fold increase in Rayleigh scattering at 1.43 mg L^{-1} iron(III) (SI Figure S3b).

Effects of Iron on Dissolved Organic Matter UV–Vis Absorption. Increases in iron(III) concentrations resulted in linear increases of a_{254} in all solutions (Figure 1a), whereas the

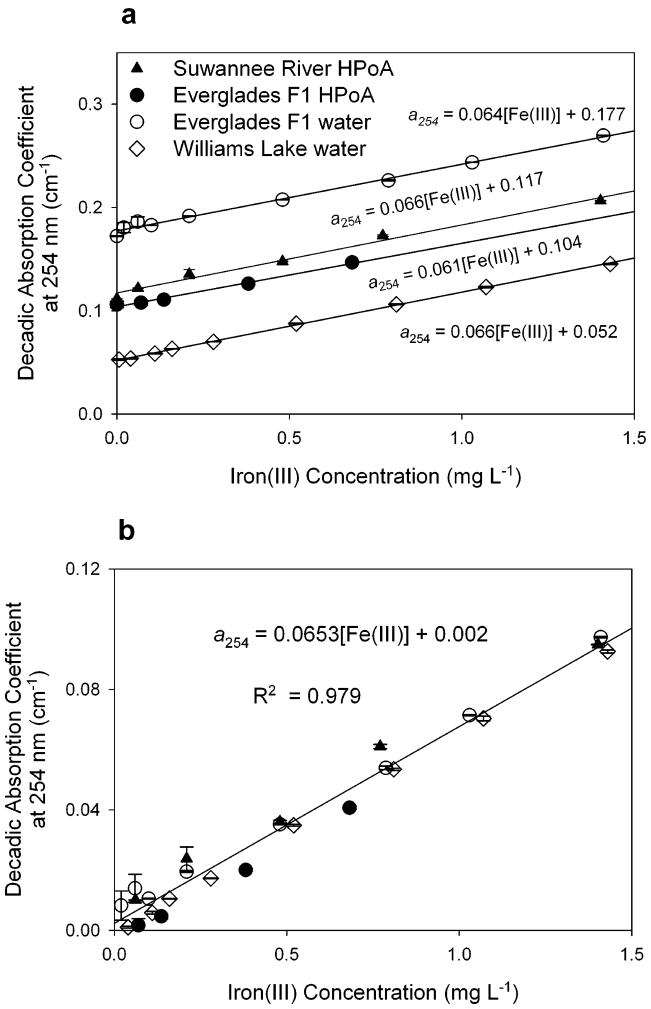

Figure 1. (a) Additive effects of iron(III) on the decadic absorption coefficient at λ = 254 nm of DOM–iron(III) systems at pH 6.7 and (b) iron(III) decadic absorption coefficients at λ = 254 nm after correction for the known absorption coefficient of DOM samples. Data points are mean values of experimental duplicates with error bars indicating the high and low values.

effects of iron(II) were negligible (data not shown). UV–vis absorption spectra of iron(III)–DOM solutions showed greater iron(III) absorption at shorter UV wavelengths (SI Figure S5a). After correcting for DOM absorption, iron(III) UV–vis spectra showed primary and secondary maxima of 206 and 271 nm, closely matching iron(III) absorption spectra collected in the absence of DOM (SI Figure S5c). Robust linear correlations were determined between iron(III) concentrations and DOM-corrected a_λ for all DOM samples ($R^2 \geq 0.88$) indicating that Beer's law is obeyed in these systems. Iron(III) absorption coefficients (ε_λ) at 254, 280, 350, and 400 nm were determined to be 6.53×10^{-2}, 5.70×10^{-2}, 3.23×10^{-2}, and 1.18×10^{-2} L mg^{-1} cm^{-1}, respectively (SI Table S2).

Greater absorption due to the presence of iron(III) resulted in considerable increases in the measured, uncorrected $SUVA_{254}$ values for all DOM samples. For example, an iron(III) concentration of 1.43 mg L^{-1} increased the measured Everglades F1 water $SUVA_{254}$ from 3.45 to 5.32 L mg_C^{-1} m^{-1}. The degree to which a given iron(III) concentration affected measured $SUVA_{254}$ varied between DOM samples due to differences in sample absorbance and DOM molar absorptivity. This observation highlights the need to correct absorbance data for iron(III). Values of S_R decreased with increasing iron(III) in all samples (SI Figure S6a) due to greater reduction in $S_{275-295}$ (i.e., less negative) compared to $S_{350-400}$. Values of E_2:E_3 also decreased with increasing iron(III) (SI Figure S6b) due to greater relative increases in a_{365} relative to a_{250}.

No changes were observed in Suwannee River HPoA absorption in the presence of iron(II) at pH < 4 (SI Figure S4b). However, elevated a_{254} were observed at pH > 4 due to iron(II) oxidation to iron(III) (SI Figure S4). For those samples containing newly formed iron(III), a_{254} values were corrected for absorption contributions of the iron(III) using the ε_{254} value in SI Table S2 (Figure S4b). This analysis was performed to ascertain if iron(III) absorption coefficients are valid for iron(III) formed via iron(II) oxidation. Data in SI Figure S4b show reasonable agreement in a_{254} between control samples (no iron) and those corrected for iron(III) (within 5.3%). UV−vis absorption spectra of iron(III) formed from iron(II) oxidation showed less pronounced absorption maxima and broader absorption spectra than those collected from iron(III) addition experiments (SI Figure S5d).

Effects of Iron on Dissolved Organic Matter Fluorescence at pH 6.7. Iron(II) addition quenched DOM fluorescence of HPoA fractions and surface water samples (Figure 2a); however, the degree of quenching varied greatly between samples. For instance, the highest iron:DOC ratio reduced Suwannee River HPoA fluorescence by 23%, whereas the fluorescence of the Williams Lake water decreased by only 7% (Figure 2a). In descending order, the degree of fluorescence quenching by iron(II) was Suwannee River HPoA > Everglades F1 water > Everglades F1 HPoA > Williams Lake water. Iron(III) addition resulted in comparable fluorescence-quenching behavior for all samples aside from Williams Lake water, which showed quenching at low iron:DOC ratios (≤0.06 mg_{Fe} mg_C^{-1}) and slight fluorescence enhancement at high iron:DOC (0.24 mg_{Fe} mg_C^{-1}; Figure 2b). Due to the oxidation or reduction of added iron, the importance of oxidation state on iron quenching was examined only qualitatively.

EEM subtractions were performed to identify and characterize changes in quenched fluorescence (EEM_{FQ}) with increasing iron concentration. Figure 3 shows EEMs and EEM_{FQ} from iron(II) titrations of Everglades F1 water. Everglades F1 water samples at low iron:DOC (Figure 3b,e) exhibited quenching in two EEM locations associated with humic-like fluorophores (A and C peaks; $\lambda_{ex}/\lambda_{em}$ = 260 nm/(380−460 nm) and 350 nm/(420−480 nm), respectively).[37] Quenching locations included shorter excitation/emission wavelength regions with increasing iron:DOC (Figure 3c,d,f,g). Iron(III) titrations yielded similar EEM_{FQ} to those observed with iron(II) (SI Figure S7). In contrast, Williams Lake water EEM_{FQ} showed low levels of quenching at all iron:DOC ratios and no distinguishable shift in quenching regions with increasing iron(II) and iron(III) (SI Figure S8). Everglades F1 HPoA experienced quenching across broad EEM regions at all iron:DOC ratios (SI Figure S9), while

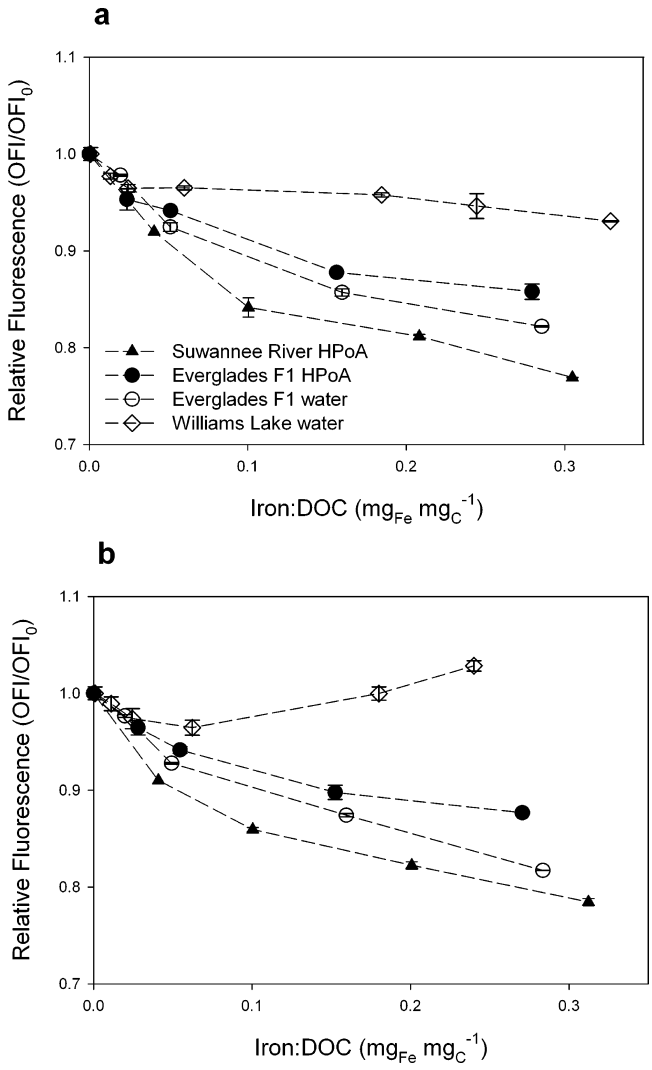

Figure 2. Relative fluorescence (OFI/OFI_0) of four DOM samples in the presence of (a) iron(II) and (b) iron(III) at pH 6.7. Data points are mean values of experimental duplicates with error bars indicating the high and low values.

Suwannee River HPoA showed trends similar to those of Everglades F1 water (SI Figure S10).

Greater iron-quenching of DOM fluorescence at long emission wavelengths (Figure 4a) increased measured FI values (Figure 4b). The measured FI of Suwannee River HPoA increased from 1.17 to 1.24 in iron(II) addition experiments at an iron:DOC ratio of 0.29 mg_{Fe} mg_C^{-1}. Iron(II) addition exhibited a similar increase in the measured FI of Everglades F1 HPoA from 1.26 to 1.34 at high iron:DOC concentration ratio. Less pronounced changes in measured FI values were observed for Everglades F1 water (ΔFI = +0.04) and Williams Lake water (ΔFI ≤ +0.02). Comparable increases in FI values were observed with iron(III). Changes in the slope of the emission peak were responsible for greater FI values.

EEMs from the iron titrations were analyzed using two PARAFAC models.[4,33] Aside from the samples with the highest iron:DOC concentration ratio (about 0.3 mg_{Fe} mg_C^{-1}), no changes were noted in the component distributions of the 13-component PARAFAC model (±1% contribution of total fluorescence).[4] When significant deviation in component distribution was observed, it was restricted to a reduction

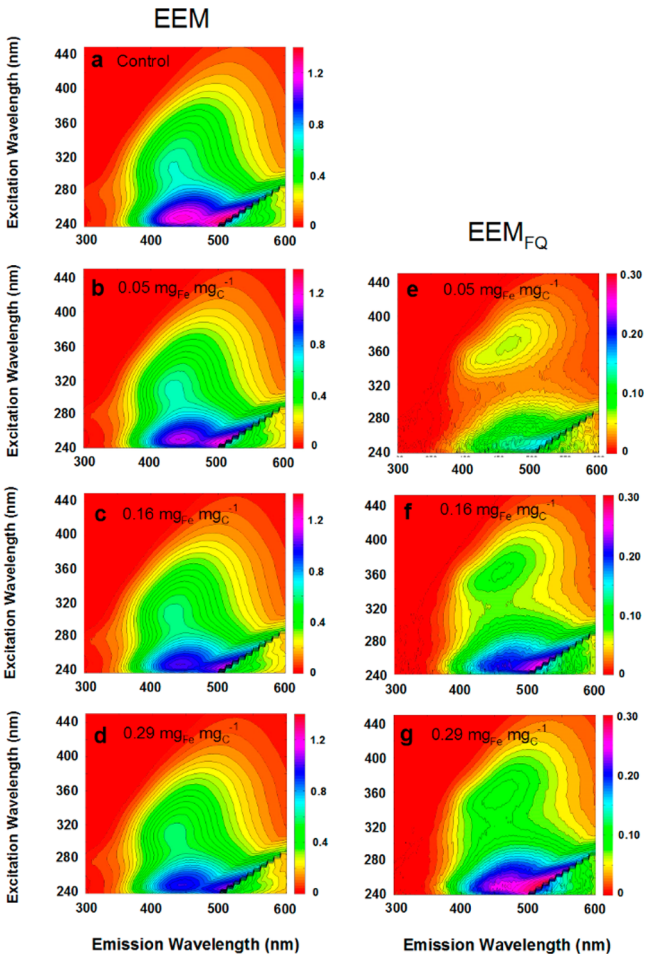

Figure 3. Excitation−emission matrices (EEMs) of Everglades F1 water with increasing iron(II) (left panel; a−d) and EEMs of fluorescence quenched (EEM$_{FQ}$) by iron(II) (pH 6.7). The iron:DOC concentration ratio is specified on each plot. Fluorescence intensities for each panel are normalized in Raman units (RU).

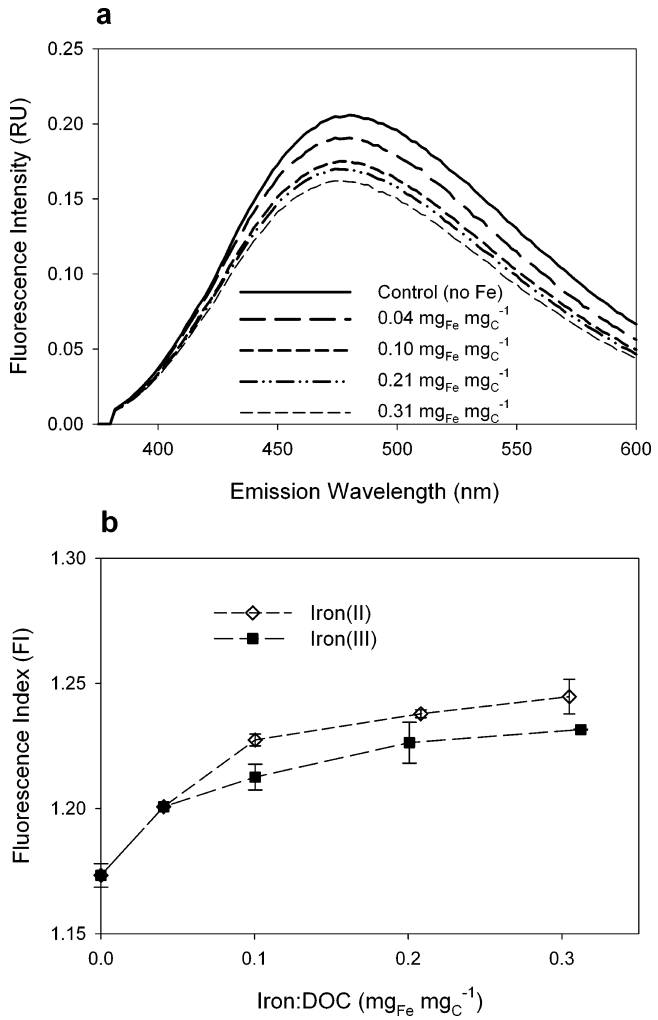

Figure 4. (a) Two-dimensional fluorescence emission 375−600 nm of Suwannee River HPoA iron(II) titrations (pH 6.7) at excitation 370 nm and (b) iron effects on the fluorescence index (FI) determined as the ratio of emission intensities measured at 470 and 520 nm with excitation at 370 nm.[4] Data points in plot b are mean values of experimental duplicates with error bars indicating the high and low values.

(≤3% of total fluorescence) in the C4 component ($\lambda_{ex}/\lambda_{em}$ ≤250 nm/≥450 nm) of HPoA samples.[4] Changes in the RI were only notable in Suwannee River HPoA samples where the measured RI decreased from 0.59 to 0.53 and 0.54 in the presence of high iron(II) and iron(III) levels, respectively, largely due to greater quenching of the C4 component. More pronounced changes in PARAFAC modeling results of Everglades F1 water and Suwannee River HPoA samples were observed using the 7-component model. Everglades F1 water exhibited a decrease in C1 (from 33% to 30% of total fluorescence) accompanied by an increase in C4 (from 16% to 18%) and C7 (from 7% to 9%). Suwannee River HPoA showed a decrease in C3 (from 20% to 17%) along with an increase in C4 (from 7% to 10%) and C7 (from 3% to 5%). The reduction in the terrestrial humic C1 and C3 contributions in these samples were responsible for the increased contribution from C4 and C7 components to the total fluorescence.

pH Effects on Iron Quenching of Suwannee River Hydrophobic Acid. Iron-free Suwannee River HPoA samples exhibited a 33% decrease in overall fluorescence intensity when acidified from pH 6.7 to 2. The greatest decrease was observed between pH 3 and 2 (SI Figure S4c). This pH dependence was also evident in EEM$_{FR}$ upon acidification (SI Figure S11). Fluorescence reduction was limited to long excitation/emission wavelengths (385 nm/475 nm) at pH 4 (SI Figure S11e) and included intermediate excitation/emission wavelengths at pH 3 (305 nm/425 nm) (Figure S11f). Measured FI values of these samples increased with pH from pH 5 to 6.7 (ΔFI = +0.07) (SI Figure S12). Solutions at pH 3 showed poor reproducibility between replicates.

Fluorescence quenching by iron was greatest at mildly acidic pH (initial pH 5−5.5), at which the total fluorescence was 88% of control samples (SI Figure S4c). Quenching by iron was negligible (total fluorescence was 98% of control samples) at low (pH ≤ 3) and circumneutral pH (pH ≥ 6) (SI Figure S4c). Iron(II) oxidation and iron(III) oxyhydroxide colloid formation at pH ≥ 6 resulted in little quenching (SI Figure S4c). Samples prepared at pH 5 exhibited moderate iron(II) oxidation but still showed fluorescence quenching despite an increase in pH (SI Figure S4). Measured FI values were most different from those of control samples at pH 4 (ΔFI = +0.13) (SI Figure S12). PARAFAC modeling results for EEMs in the presence and absence of iron show deviation with pH (SI Table S3).

dx.doi.org/10.1021/es502670r | Environ. Sci. Technol. 2014, 48, 10098−10106

DISCUSSION

Effects of Iron on Dissolved Organic Matter UV−vis Absorption. The negligible effects of iron(II) on DOM absorption coefficients are consistent with past findings.[13] Similarly, the linear relationship between iron(III) concentration and a_{254} observed across a range of DOM samples (Figure 1) agrees with previous iron(III) addition experiments.[3,14] The iron(III) ε_{350} (SI Table S2) is in good agreement (<8% difference) with that reported in other DOM-containing systems.[14] However, iron(III) absorption spectra differed between solutions with added iron(III) and those where iron(III) formed from iron(II) oxidation (SI Figure S5). When iron(III) is directly added to DOM solutions, the resulting iron(III) absorption spectra are similar to those reported for aqueous $FeOH^{2+}$ and $Fe(OH)_2^+$ species.[19] In contrast, iron(III) generated from iron(II) oxidation showed absorption spectra indicative of a combination of iron(III) oxyhydroxide colloids[7,38] and aqueous iron(III) species.[19] Although differences in iron(III) absorption spectra are apparent, the differences were not substantial enough to influence the application of a correction factor based on the concentration of iron(III). For instance, iron(III)-corrected a_{254} values of Suwannee River HPoA were in good agreement with those of control samples across a range of iron:DOC concentration ratios and pH values (SI Figure S4b). This result confirms that iron(III) absorption coefficients (SI Table S2) are suitable for iron(III) correction of environmental samples where iron redox cycling,[7,35] iron:DOC concentration ratio,[8] and pH likely control the distribution of iron(III) between dissolved and colloidal phases.

Empirically correcting the a_λ for iron(III) only requires knowledge of the iron(III) concentration. Alternatively, an iron(III) reduction method[13] requires pH adjustment for reductant efficiency and UV−vis correction for absorption by the reductant and could pose issues for redox-sensitive fluorescence measurements.[4,36] The iron(III) correction approach proposed here was verified for samples with iron(III):DOC concentration ratios ≤ 0.35 mg_{Fe} mg_C^{-1}. UV−vis interference by iron(III) is suspect in surface waters that are acidic, collected from peatlands,[39] drain watersheds with iron-rich minerals,[8] or exchange with suboxic, iron(II)-rich waters (e.g., groundwater exchange[40] or lake turnover[11,12]).

Failing to correct absorption coefficients for iron(III) will result in overestimation of UV−vis absorption values. In the case of Everglades F1 water with the addition of 1.43 mg L^{-1} iron(III), the measured $SUVA_{254}$ (5.32 L mg_C^{-1} m^{-1}) was outside the range of values common for surface water samples (1.0−5.0 L mg_C^{-1} m^{-1}).[41] It is important to note that iron(III) interference is still of concern when the measured $SUVA_{254}$ is within the range of feasible values. Although iron(III) absorption is greater at shorter UV wavelengths (SI Figure S5), $SUVA_{280}$ values were more prone to iron(III) interference than $SUVA_{254}$ due to greater absorption decay of DOM relative to iron(III) with increasing wavelength. S_R and E_2:E_3 were also influenced by iron(III), albeit to a lesser degree than $SUVA_{254}$. Measured S_R and E_2:E_3 values in the presence of iron(III) inferred DOM of greater bulk molecular weight[5] and relative size (SI Figure S6).[26]

Effects of Iron on Dissolved Organic Matter Fluorescence. Decreases of DOM fluorescence in the presence of iron(II) are attributed to ground-state iron(II)−DOM interactions (Figure 2). No increase in Rayleigh scattering was observed with increasing iron(II) at pH 6.7 (SI Figure S3a), and quenching was eliminated at pH $\leq$ 3 (SI Figure S4c) due to proton competition for DOM functional groups. These observations support a static quenching mechanism.[15] Under oxic conditions, there is evidence of iron(II)−DOM complexation controlling iron(II) oxidation rates.[7,8,42] Similar interactions are likely responsible for observed iron(II) quenching in this study. Alternatively, iron(II) quenching through dynamic (i.e., collisional) interactions has not been observed with model fluorophores;[15,43] therefore, we consider dynamic quenching to be unlikely for Fe(II)−DOM interaction. This finding contradicts those of Pullin et al.,[18] who observed no significant quenching by iron(II). However, they employed a chemical reductant to prevent iron(II) oxidation. This may have masked iron(II) quenching due to the expected increase in DOM fluorescence yield of reduced DOM.[4,36]

The effects of iron(III) on DOM fluorescence showed contrasting behavior between samples where iron(III) was directly added (Figure 2b) and those where iron(III) formed from iron(II) oxidation (SI Figure S4c). When added directly to DOM solution, iron(III) quenching was comparable to that of iron(II) addition (Figure 2) and in agreement with observations reported in previous studies.[16−18,23,44] In contrast, almost no quenching was observed when iron(III) formed from iron(II) oxidation at pH 6.7 (SI Figure S4c). These findings are likely due to the importance of the initial iron oxidation state on the formation of iron(III) oxyhydroxide colloids. Pullin and Cabaniss[7] observed the formation of more iron(III) oxyhydroxide colloids upon iron(II) oxidation in comparison to iron(III) addition in the presence of DOM; these authors suggest that multiple pathways for iron(III) oxyhydroxide colloid formation may exist. In our study, no quenching was observed when iron(III) formed from iron(II) oxidation (pH 6.7) due to the greater yield of iron(III) oxyhydroxide colloids and, therefore, less iron(III) available for static quenching. Analogous samples equilibrated at pH 5, where near-complete iron(II) oxidation was also observed (SI Figure S4a), showed moderate levels of quenching (SI Figure S4c). This is likely due to slower rates of iron(III) hydrolysis at lower pH, which has been observed to influence static quenching by iron(III).[15,17] The conflicting effects of iron(III) on DOM fluorescence, based on the form of addition, complicates predicting iron(III) interferences in environmental samples.

Although iron(III) oxyhydroxide colloids do not participate in static quenching, promoting the formation of iron(III) oxyhydroxide colloids is not a viable approach to minimize fluorescence interferences for two reasons. First, the sorption of hydrophobic DOM to suspended iron(III) oxyhydroxide colloids[10] can influence DOM fluorescence.[45] DOM fractionation is likely responsible for elevated FI values measured of Suwannee River HPoA samples with high levels of iron(III) oxyhydroxide colloids (SI Figure S12), even though no significant quenching was observed in these samples (SI Figure S4c). Second, iron(III) oxyhydroxide colloids,[17] and other metal colloids,[24] can enhance fluorescence for some DOM samples. For instance, small levels of fluorescence enhancement in Williams Lake water at high iron:DOC (Figure 2b) were likely a result of iron(III) oxyhydroxide colloids. This phenomenon was likely observed in Williams Lake water, as opposed to the other DOM samples, because DOM of lower $SUVA_{254}$ is less surface-active with regard to particle formation.[46] The complexity of iron(III) speciation in the environment hinders the use of techniques, such as cation

exchange or the addition of a complexing ligand (e.g., ethylenediaminetetraacetic acid (EDTA)), to eliminate iron(III) interferences because these methods require the predominance of dissolved ions to be effective.

The contrasting iron-quenching behaviors of the four DOM samples can be attributed to differences in DOM composition. Preferential iron-quenching in humic A and C peak regions[37] of HPoA samples (SI Figures S9 and S10) could be the result of iron complexation by fluorophores of higher molecular weight or greater sensitivity of these fluorophores to static quenching. Similar iron(III) quenching behavior was observed with soil organic matter leachates.[23] Iron quenching was not observed in fluorescence regions associated with simple phenolic fluorophores (e.g., $\lambda_{ex}/\lambda_{em}$ 270 nm/310 nm) and indole-containing compounds (e.g., $\lambda_{ex}/\lambda_{em}$ 260 nm/340 nm),[4,47] even in Williams Lake water, which has stronger autochthonous fluorescence signatures (SI Figure S1). Greater overall iron-quenching of Everglades F1 water in comparison to Everglades F1 HPoA (Figure 2) suggests that certain fluorophores exhibit varying sensitivity to iron aside from properties of aromaticity or molecular weight. These differences were not explained by differences in trace metal concentrations (SI Table S1).[17,21,22]

Fluorescence indices proved susceptible to interferences due to iron quenching and pH effects. HPoA samples exhibited the greatest increase in FI values from iron due to preferential quenching at high-emission wavelengths (Figure 4). The effects of iron on FI values were greatest (ΔFI = +0.13 FI units) at pH 4 (SI Figure S12). In all cases, the shifts were toward more positive values that infer DOM of greater autochthonous origin.[2] These results do not invalidate the use of FI to infer DOM source[2] but draw attention to the sensitivity of indices defined at discrete wavelength pairs. Solution pH and iron concentration should be monitored and reported when conclusions are drawn on differences in FI values $\leq$0.10 FI units.

FI values of iron-containing samples acidified to pH 2 were consistent with those of control samples, which supports the acidification protocol put forth by McKnight et al.[2] to minimize metal effects on fluorescence indices. However, a serious limitation associated with obtaining data at low pH is that EEMs of iron-free Suwannee River HPoA showed nonuniform decreases in fluorescence upon acidification (SI Figure S11). The greatest decreases occurred between pH 3 and 2 (SI Figures S4c and S11g), which is below the pK_a of most carboxyl functional groups in DOM.[48] One possible explanation is the protonation of excited-state phenols at pH < 3, which are strong acids in the excited state.[49] Common phenol moieties in DOM show considerable overlap in fluorescence peak locations,[16] which would explain the ubiquitous fluorescence decrease observed at pH 2 (SI Figure S11g). The observed nonuniform decrease in DOM fluorescence with acidification is corroborated by other studies.[16,30,50]

The deviation in PARAFAC modeling results observed upon acidification were proportional, or greater (SI Table S3), than those observed in iron titrations. The effects of iron(II) and iron(III) on PARAFAC component distributions were relatively small, or negligible, due to the overlap between multiple PARAFAC components and iron-quenching locations. However, results from the 7-component model showed an increase in component contributions to the total fluorescence as a consequence of the quenching of other components by iron. This observation highlights an important characteristic of PARAFAC modeling. PARAFAC component distributions are based on relative, not absolute, fluorescence intensities. Therefore, it should not be assumed that an increase in one component's contribution to the total fluorescence means there is "more" of this component.

Practical Implications. UV−vis absorption and fluorescence spectroscopy are growing in popularity as tools to monitor DOM concentration, composition, and reactivity. While UV−vis absorption parameters based on absolute (e.g., $SUVA_{254}$; spectral slope), as opposed to relative (e.g., S_R, E_2:E_3), absorption proved more susceptible to iron(III) interference, iron(III) absorption coefficients provided here are a reasonable correction method for DOM UV−vis absorption measurements regardless of DOM composition. However, the nonconservative behavior of DOM fluorescence in the presence of iron illustrates the inherent complexities of this method. Other environmentally relevant metals, principally manganese and aluminum,[17,23] can influence DOM fluorescence and are worthy of investigation. The results presented here call into question the efficacy of fluorescence-quenching methods to derive metal−DOM stability constants.[21−23,34] Similar quenching strengths were observed by iron regardless of oxidation state (Figure 2), which would not be predicted based on the hierarchy of iron−DOM binding strength (iron(III) > iron(II)) observed under oxygen-free conditions.[8,42] This lack of sensitivity is most evident when comparing metal−DOM stability constants reported for major (Al(III), Fe(III)) and trace metals (Cu(II), Hg(II)) using fluorescence quenching. Regardless of the metal ion, the reported stability constants span a narrow range of values ($\sim 4 < \log K < 6.7$),[21−23] which do not agree with the much broader range or order of stability constants established using other approaches.[51,52] Another issue with the use of fluorescence-quenching methods arises from the complex set of factors that control DOM optical properties, including both chemical interactions (e.g., intramolecular interactions)[53] and environmental conditions (e.g., pH and redox status).[4,16,30,36,50] In addition, nonfluorescent ligands are not accounted for using the fluorescence-quenching approach.

Finally, the presence of iron could also have implications for the use of in situ fluorescence sensors in freshwater systems. These sensors measure the fluorescence of the humic C peak ($\lambda_{ex}/\lambda_{em}$ = (350−370 nm)/(430−460 nm)), and provide an inexpensive, high-resolution proxy for DOC concentration and DOM quality.[6] Iron could influence in situ fluorescent DOM measurements in two ways. First, both dissolved iron(III) and iron(III) oxyhydroxide colloids could attenuate excitation and emission signals through absorbance and light scattering. Second, quenching by both iron(II) and iron(III) could reduce DOM fluorescence emission. Commercially available in situ probes make fluorescent DOM measurements in EEM regions where quenching by iron was observed.[6] The magnitude of iron effects on in situ fluorescent DOM measurements should be assessed in cases where the presence of iron is likely.

■ ASSOCIATED CONTENT

Supporting Information

EEMs and background chemistry of DOM samples (Figure S1, Table S1), estimates of electron-donating capacity of DOM samples, iron(III)−DOM equilibration kinetics and matrix effects (Figure S2), details on DOM optical measurements, fluorescence Rayleigh scattering (Figure S3), results for Suwannee River HPoA samples at pH 2−6.7 (Figure S4), UV absorption spectra of iron(III)−DOM solutions (Figure S5), iron(III) absorption coefficients (Table S2), effects of

iron(III) on UV−vis absorption parameters (Figure S6), EEMs of fluorescence quenched (Figures S7−S10), pH effects on DOM fluorescence in the presence and absence of iron (Figures S11 and S12, Table S3), and accompanying references. This material is available free of charge via the Internet at http://pubs.acs.org.

AUTHOR INFORMATION

Corresponding Author

*Phone: (303) 541-3036; fax: (303) 541-3084; e-mail: graiken@usgs.gov.

Notes

The authors declare no competing financial interest.

ACKNOWLEDGMENTS

We acknowledge K. Butler for assistance with sample analysis and data processing. This research was supported by the U.S. Geological Survey National Research Program and the Department of Energy Subsurface Biogeochemical Research Program (Grant DE-SC0001766). Any use of trade, firm, or product names is for descriptive purposes only and does not imply endorsement by the U.S. Government.

REFERENCES

(1) Chin, Y. P.; Aiken, G. R.; O'Loughlin, E. Molecular weight, polydispersity, and spectroscopic properties of aquatic humic substances. *Environ. Sci. Technol.* **1994**, *28*, 1853−1858.

(2) McKnight, D. M.; Boyer, E. W.; Westerhoff, P. K.; Doran, P. T.; Kulbe, T.; Andersen, D. T. Spectrofluorometric characterization of dissolved organic matter for indication of precursor organic material and aromaticity. *Limnol. Oceanogr.* **2001**, *46*, 38−48.

(3) Weishaar, J. L.; Aiken, G. R.; Bergamaschi, B. A.; Fram, M. S.; Fujii, R.; Mopper, K. Evaluation of specific ultraviolet absorbance as an indicator of the chemical composition and reactivity of dissolved organic carbon. *Environ. Sci. Technol.* **2003**, *37*, 4702−4708.

(4) Cory, R. M.; McKnight, D. M. Fluorescence spectroscopy reveals ubiquitous presence of oxidized and reduced quinones in dissolved organic matter. *Environ. Sci. Technol.* **2005**, *39*, 8142−8149.

(5) Helms, J. R.; Stubbins, A.; Ritchie, J. D.; Minor, E. C. Absorption spectral slopes and slope ratios as indicators of molecular weight, source, and photobleaching of chromophoric dissolved organic matter. *Limnol. Oceanogr.* **2008**, *53*, 955−969.

(6) Downing, B. D.; Pellerin, B. A.; Bergamaschi, B. A.; Saraceno, J. F.; Kraus, T. E. C. Seeing the light: The effects of particles, dissolved materials, and temperature on in situ measurements of DOM fluorescence in rivers and streams. *Limnol. Oceanogr.: Methods* **2012**, *10*, 767−775.

(7) Pullin, M. J.; Cabaniss, S. E. The effects of pH, ionic strength, and iron-fulvic acid interactions on the kinetics of non-photochemical iron transformations. I. Iron(II) oxidation and iron(III) colloid formation. *Geochim. Cosmochim. Acta* **2003**, *67*, 4067−4077.

(8) Gaffney, J. W.; White, K. N.; Boult, S. Oxidation state and size of Fe controlled by organic matter in natural waters. *Environ. Sci. Technol.* **2008**, *42*, 3575−3581.

(9) Pédrot, M.; Boudec, A. L.; Davranche, M.; Dia, A.; Henin, O. How does organic matter constrain the nature, size and availability of Fe nanoparticles for biological reduction? *J. Colloid Interface Sci.* **2011**, *359*, 75−85.

(10) Meier, M.; Namjesnik-Dejanovic, K.; Maurice, P. A.; Chin, Y. P.; Aiken, G. R. Fractionation of aquatic natural organic matter upon sorption to goethite and kaolinite. *Chem. Geol.* **1999**, *157*, 275−284.

(11) Bertilsson, S.; Tranvik, L. J. Photochemical transformation of dissolved organic matter in lakes. *Limnol. Oceanogr.* **2000**, *45*, 753−762.

(12) Maloney, K. O.; Morris, D. P.; Moses, C. O.; Osburn, C. L. The role of iron and dissolved organic carbon in the absorption of ultraviolet radiation in humic lake water. *Biogeochemistry* **2005**, *75*, 393−407.

(13) Doane, T. A.; Horwáth, W. R. Eliminating interference from iron(III) for ultraviolet absorbance measurements of dissolved organic matter. *Chemosphere* **2010**, *78*, 1409−1415.

(14) Xiao, Y. H.; Sara-Aho, T.; Hartikainen, H.; Vähätalo, A. V. Contribution of ferric iron to light absorption by chromophoric dissolved organic matter. *Limnol. Oceanogr.* **2013**, *58*, 653−662.

(15) Waite, T. D.; Morel, F. M. M. Ligand exchange and fluorescence quenching studies of the fulvic acid-iron interaction: Effects of pH and light. *Anal. Chim. Acta* **1984**, *162*, 263−274.

(16) Senesi, N. Molecular and quantitative aspects of the chemistry of fulvic acid and its interactions with metal ions and organic chemicals: Part II. The fluorescence spectroscopy approach. *Anal. Chim. Acta* **1990**, *232*, 77−106.

(17) Cabaniss, S. E. Synchronous fluorescence spectra of metal-fulvic acid complexes. *Environ. Sci. Technol.* **1992**, *26*, 1133−1139.

(18) Pullin, M. J.; Anthony, C.; Maurice, P. A. Effects of iron on the molecular weight distribution, light absorption, and fluorescence properties of natural organic matter. *Environ. Eng. Sci.* **2007**, *24*, 987−997.

(19) Stefánsson, A. Iron(III) hydrolysis and solubility at 25 °C. *Environ. Sci. Technol.* **2007**, *41*, 6117−6123.

(20) Maurer, F.; Christl, I.; Kretzschmar, R. Reduction and reoxidation of humic acid: Influence on spectroscopic properties and proton binding. *Environ. Sci. Technol.* **2010**, *44*, 5787−5792.

(21) Plaza, C.; Brunetti, G.; Senesi, N.; Polo, A. Molecular and quantitative analysis of metal ion binding to humic acids from sewage sludge and sludge-amended soils by fluorescence spectroscopy. *Environ. Sci. Technol.* **2006**, *40*, 917−923.

(22) Yamashita, Y.; Jaffé, R. Characterizing the interactions between trace metals and dissolved organic matter using excitation-emission matrix and parallel factor analysis. *Environ. Sci. Technol.* **2008**, *42*, 7374−7379.

(23) Ohno, T.; Amirbahman, A.; Bro, R. Parallel factor analysis of excitation−emission matrix fluorescence spectra of water soluble soil organic matter as basis for the determination of conditional metal binding parameters. *Environ. Sci. Technol.* **2007**, *42*, 186−192.

(24) Lakowicz, J. R. *Principles of Fluorescence Spectroscopy*, 3rd ed.; Springer Science+Business Media: New York, 2006.

(25) Stedmon, C. A.; Markager, S.; Bro, R. Tracing dissolved organic matter in aquatic environments using a new approach to fluorescence spectroscopy. *Mar. Chem.* **2003**, *82*, 239−254.

(26) De Haan, H.; De Boer, T. Applicability of light absorbance and fluorescence as measures of concentration and molecular size of dissolved organic carbon in humic Lake Tjeukemeer. *Water Res.* **1987**, *21*, 731−734.

(27) Aiken, G. R.; McKnight, D. M.; Thorn, K. A.; Thurman, E. M. Isolation of hydrophilic organic acids from water using nonionic macroporous resins. *Org. Geochem.* **1992**, *18*, 567−573.

(28) Aeschbacher, M.; Graf, C.; Schwarzenback, R. P.; Sander, M. Antioxidant properties of humic substances. *Environ. Sci. Technol.* **2012**, *46*, 4916−4925.

(29) To, T. B.; Nordstrom, D. K.; Cunningham, K. M.; Ball, J. W.; McCleskey, R. B. New method for the direct determination of dissolved Fe(III) concentration in acid mine waters. *Environ. Eng. Sci.* **1999**, *33*, 807−813.

(30) Mobed, J. J.; Hemmingsen, S. L.; Autry, J. L.; McGown, L. B. Fluorescence characterization of IHSS humic substances: Total luminescence spectra with absorbance correction. *Environ. Sci. Technol.* **1996**, *30*, 3061−3065.

(31) Fujii, M.; Imaoka, A.; Yoshimura, C.; Waite, T. D. Effects of molecular composition of natural organic matter on ferric iron complexation at circumneutral pH. *Environ. Sci. Technol.* **2014**, *48*, 4414−4424.

(32) Miller, M. P.; McKnight, D. M.; Cory, R. M.; Williams, M. W.; Runkel, R. L. Hyporheic exchange and fulvic acid redox reactions in an alpine stream/wetland ecosystem, Colorado Front Range. *Environ. Sci. Technol.* **2006**, *40*, 5943−5949.

(33) Cawley, K. M.; Butler, K. D.; Aiken, G. R.; Larsen, L. G.; Huntington, T. G.; McKnight, D. M. Identifying fluorescent pulp mill effluent in the Gulf of Maine and its watershed. *Mar. Pollut. Bull.* **2012**, *64*, 1678−1687.
(34) Ryan, D. K.; Weber, J. H. Fluorescence quenching titration for determination of complexing capacities and stability constants of fulvic acid. *Anal. Chem.* **1982**, *54*, 986−990.
(35) Pullin, M. J.; Cabaniss, S. E. The effects of pH, ionic strength, and iron-fulvic acid interactions on the kinetics of non-photochemical iron transformations. II. The kinetics of thermal reduction. *Geochim. Cosmochim. Acta* **2003**, *67*, 4079−4089.
(36) Klapper, L.; McKnight, D. M.; Fulton, J. R.; Blunt-Harris, E. L.; Nevin, K. P.; Lovley, D. R.; Hatcher, P. G. Fulvic acid oxidation state detection using fluorescence spectroscopy. *Environ. Sci. Technol.* **2002**, *36*, 3170−3175.
(37) Coble, P. G. Characterization of marine and terrestrial DOM in seawater using excitation-emission matrix spectroscopy. *Mar. Chem.* **1996**, *51*, 325−346.
(38) Sherman, D. M.; Waite, T. D. Electronic spectra of Fe^{3+} oxides and oxide hydroxides in the near IR to near UV. *Am. Mineral.* **1985**, *70*, 1262−1269.
(39) Moore, T. R. Dissolved iron and organic matter in northern peatlands. *Soil Sci.* **1988**, *145*, 70−76.
(40) Ingri, J.; Malinovsky, D.; Rodushkin, I.; Baxter, D. C.; Widerlund, A.; Andersson, P.; Gustafsson, Ö.; Forsling, W.; Öhlander, B. Iron isotope fractionation in river colloidal matter. *Earth Planet. Sci. Lett.* **2006**, *245*, 792−798.
(41) Spencer, R. G. M.; Butler, K. D.; Aiken, G. R. Dissolved organic carbon and chromophoric dissolved organic matter properties of rivers in the USA. *J. Geophys. Res.: Biogeosci.* **2012**, *117*, No. G03001, DOI: 10.1029/2011JG001928.
(42) Jackson, A.; Gaffney, J. W.; Boult, S. Subsurface interactions of Fe(II) with humic acid or landfill leachate do not control subsequent iron(III) (hydr)oxide production at the surface. *Environ. Sci. Technol.* **2012**, *46*, 7543−7550.
(43) Cha, K. W.; Park, K. W. Determination of iron(III) with salicylic acid by the fluorescence quenching method. *Talanta* **1998**, *46*, 1567−1571.
(44) Yan, M.; Benedetti, M. F.; Korshin, G. V. Study of iron and aluminum binding to Suwannee River fulvic acid using absorbance and fluorescence spectroscopy: comparison of data interpretation based on NICA-Donnan and Stockholm humic models. *Water Res.* **2013**, *47*, 5439−5446.
(45) Banaitis, M. R.; Waldrip-Dail, H.; Diehl, M. S.; Holmes, B. C.; Hunt, J. F.; Lynch, R. P.; Ohno, T. Investigating sorption-driven dissolved organic matter fractionation by multidimensional fluorescence spectroscopy and PARAFAC. *J. Colloid Interface Sci.* **2006**, *304*, 271−276.
(46) Deonarine, A.; Lau, B. L. T.; Aiken, G. R.; Ryan, J. N.; Hsu-Kim, H. Effects of humic substances on precipitation and aggregation of zinc sulfide nanoparticles. *Environ. Sci. Technol.* **2011**, *45*, 3217−3223.
(47) Maie, N.; Scully, N. M.; Pisani, O.; Jaffé, R. Composition of a protein-like fluorophore of dissolved organic matter in coastal wetland and estuarine ecosystems. *Water Res.* **2007**, *41*, 563−570.
(48) Perdue, M. E.; Acidic functional groups of humic substances. In *Humic substances in soil, sediment, and water: Geochemistry, isolation, and characterization*; Aiken, G. R., McKnight, D. M., Wershaw, R. L., MacCarthy, P., Eds.; John Wiley & Sons: New York, 1985; pp 493−526.
(49) Wolfbeis, O. S.; Begum, M.; Hochmuth, P. An unusual excited state species of ortho-hydroxy-cinnamic acid. *Photochem. Photobiol.* **1986**, *44*, 551−554.
(50) Spencer, R. G. M.; Bolton, L.; Baker, A. Freeze/thaw and pH effects on freshwater dissolved organic matter fluorescence and absorbance properties from a number of UK locations. *Water Res.* **2007**, *41*, 2941−2950.
(51) Batchelli, S.; Muller, F. L. L.; Chang, K. C.; Lee, C. L. Evidence for strong but dynamic iron−humic colloidal associations in humic-rich coastal waters. *Environ. Sci. Technol.* **2010**, *44*, 8485−8490.
(52) Tipping, E. *Cation Binding by Humic Substances*; Cambridge University Press: Cambridge, U.K., 2002.
(53) Del Vecchio, R.; Blough, N. V. On the origin of the optical properties of humic substances. *Environ. Sci. Technol.* **2004**, *38*, 3885−3891.